The Nucleus, **45** (1-2) 2008 : 1-5

The Nucleus
A Quarterly Scientific Journal of
Pakistan Atomic Energy Commission
NCLEAM, ISSN 0029-5698

FABRICATION AND CONTACTING INDIVIDUAL GOLD NANOWIRES

*S. KARIM and W. ENSINGER[1]

Physics Division, Directorate of Science, PINSTECH, P.O. Nilore, Islamabad, Pakistan

[1]Institute of Material and Earth Science, Darmstadt University of Technology, Darmstadt, Germany

(Received February 7, 2008 and accepted in revised form April 17, 2008)

Gold nanowires with diameters ranging from 80 to 320 nm are electrochemically fabricated in etched single-pore membranes. By means of two macroscopic planar electrodes on either side of the membrane, single nanowires are successfully contacted. The fabrication and contacting method is presented and the measured resistance-versus-diameter behavior of the nanowires is discussed, considering electron scattering both at the wire surface and at the grain boundaries.

Keywords : Electrodeposition, Template method, Nanowires, Size effect, Electrical resistivity

1. Introduction

Metallic nanowires are regarded as essential components for the development of nanoelectronic devices. Their electrical resistivity, being one of the most important properties in electrical applications, is the subject of intense theoretical and experimental investigations [1, 2]. Besides this, they are considered excellent subjects to investigate how the properties of solids deviate from macroscopic behaviour when their dimensions are comparable to characteristic length scales such as the electron mean free path [1, 3, 4]. The electrical properties of large macroscopic wires, the so-called diffusive transport regime, are well established. The resistance *R* follows the relationship $R = \rho L/A$. ρ is the specific electrical resistivity, and *L* and A are the sample length and cross-sectional area, respectively. If the wire size is comparable to the Fermi wavelength, quantization effects due to the confinement of the electronic wave functions are expected. Wires exhibit discrete resistance values described by the Landauer–Büttiker formalism [5]. The wires that are produced in this work can be attributed to an intermediate, the so-called mesoscopic regime. In this regime the diameters are comparable to the electron mean free path (l_e). Electron transport is strongly influenced by two mechanisms: scattering (elastic or inelastic) of the electrons at the wire surface, described by Dingle *et al.* [6] and Fuchs [7], and that at the grain boundaries, described by Mayadas and Shatzkes [8]. Both effects contribute to an increase of the nanowire resistivity compared to the bulk resistivity.

In most cases, the properties were measured either by contacting a plurality of wires embedded in templates [3, 9] or by lithographically fabricating and contacting single nanowires [4]. The absolute value of resistivity of single wires cannot be obtained from investigation on wire ensembles, while in the lithography based approach manipulation of crystallinity of wires is not possible. Recently, Satti et al. prepared Au nanowires employing DNA as the template and measured the electrical characteristics using electron beam lithography to write electrical contacts to individual wires [10]. Valizadeh et al. electrochemically synthesized Au nanowires in polycarbonate membranes and subsequently used focused ion beam techniques to create electrical contacts [11].

In this work, we fabricated individual gold nanowires by electrochemical deposition in single-pore membranes and electrical transport properties have been measured while keeping the individual wires embedded in the templates. Previously, this method has been used for contacting single Bi and Cu nanowires [12, 13]. This technique circumvents the necessity of manipulation of individual nanowire or lithographic techniques, thus, making the method very simple and accessible to a large number of laboratories.

2. Experimental

Polymer foils (Makrofol, Bayer Leverkusen) were irradiated normal to the surface by U ions of energy 11.4 MeV/u at the UNILAC accelerator of GSI (Darmstadt, Germany) through a circular

* Corresponding author : s.karim@gsi.de

aperture with 100 μm radius in an aluminum mask of 0.2 mm thickness. By employing ion fluxes of 10^3–10^4 ions cm^{-2} s^{-1}, on average, one ion per second passes through the aperture and hits the sample. This small rate gives enough time to switch off the beam, using a fast chopper, as soon as a semiconductor detector placed behind the sample has registered the single-ion hit.

Subsequently, the latent tracks created by the single-ion on their way through the foils were etched to cylindrical pores in a two-compartment compression-sealed cell. We irradiated each foil prior to etching with UV light, thus increasing the track etching selectivity (i.e., the track-to-bulk etch-rate ratio, V_T/V_B. On each side of the polymer membrane 2M NaOH solution was filled, Au electrodes were immersed, and a constant potential of 2 V was applied. The etching was performed at 60 °C, and the pore evolution was monitored by measuring the electrical current through the cell [14].

The pore diameter increases directly proportionally to the final etching time. The process was stopped by rinsing the pore with distilled water. Subsequently, the conductivity of the pore was determined. For this purpose, the chambers were filled with a 1 M KCl solution at room temperature, applying 1 V between the two Ag/AgCl electrodes, placed one on each side of the membrane. The effective pore diameter *d* is calculated assuming cylindrical geometry, and using the following equation,

$$d = \sqrt{\frac{4LI}{\pi\sigma E}}$$

where *L* is the pore length corresponding to foil thickness, *I* is the measured current, *E* is the applied voltage, and σ is the conductivity of the 1M KCl solution ($10.2\ Sm^{-1}$ at $20\ ^oC$).

After etching, the sample was taken out of the cell, rinsed, and dried, and a gold layer was sputtered on one side using an Edwards Sputter Coater S150 B. Afterward, the foil was returned to its former place in the cell. A Cu layer was then deposited electrochemically onto the gold. This thin layer acted as cathode during the subsequent electrodeposition of gold. During deposition of the wires, we employed the ammonium gold (I) sulfite electrolyte at T = 50 °C, and E = -0.8 V using a thin Au rod as the anode [15, 16]. When the wire reaches the membrane surface, a three dimensional structure or cap starts to grow on top. At this point in time, the electrodeposition process is stopped, the sample removed from the cell and processed for electrical contacting.

3. Results and Discussion

3.1. Etching of single cylindrical pores:

Current evolution during etching of a single track is displayed as a function of time in Fig. 1. The inset in this figure shows the current during etching on a magnified scale. In the first few minutes no current is recorded, as soon as the track is dissolved and an open channel has been created, a finite current is recorded which increases with time because of enlarging pore diameter. The breakthrough time indicated by a sharp current increase in Fig. 1 is 6.5 min, and the track-etching rate amounts to 2.3 μm/min. For individual single pores etched from both sides, the opening time varied from 3 to 9 min, which correspond to a track-etching rate V_T ranging from 1.7 to 5 μm/min. The bulk etch rate V_B of polycarbonate is about 1 nm/min, resulting in $V_T/V_B > 10^3$. The etching behavior of a single ion track is influenced by the fact that the energy loss of the ion along its path is not smooth but fluctuates stochastically. Furthermore, it also depends on the inhomogeneous structure of the polycarbonate foil originating from the production procedure. As a result, each single track showed individual behavior with regard to the time needed for perforation [17].

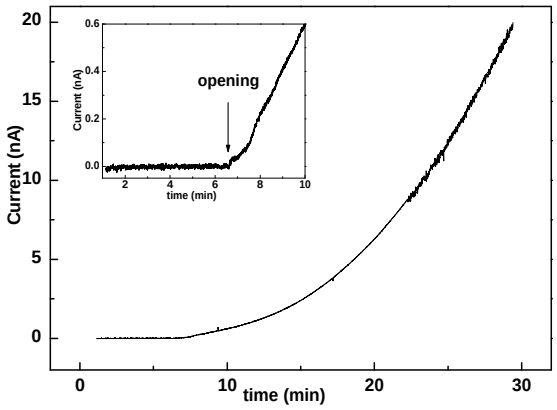

Figure 1: Current-versus-time curve recorded during etching of a single pore. Inset shows the current on a magnified scale during initial few minutes of etching.

3.2. Electrodeposition of single wire

The current versus time curve recorded during the electrodeposition of a wire of diameter 200 nm is presented in Fig. 2. The curve in this figure can

be divided into two steps. In the beginning, the current is steady which corresponds to the actual filling of the pores with the material. The beginning of the second step represents the moment when the pores are completely filled and cap starts to grow on the surface of the membrane. The strong increase of the current during this step is due to the increase in deposition surface when compared to phenomena taking place inside the pores.

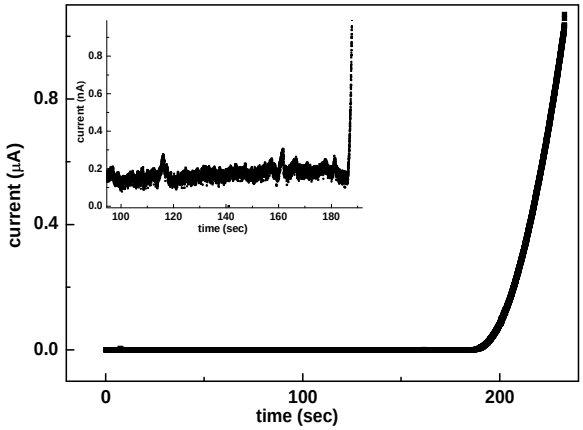

Figure 2. Current-versus-time curve recorded during Au electrodeposition into pores of diameter 200 nm. Inset shows the *I(t)* behavior on a magnified scale.

3.3 Electrical characteristics of the wires

All the electrical measurements were performed in a two-electrode arrangement. The single wires were contacted electrically by coating the cap with an additional gold layer and placing the membrane containing the wire between two copper plates. The upper electrode is caved in its centre for avoiding direct pressure on the cap. The experimental setup used for electrically contacting the single wires is schematically displayed in Fig. 3.

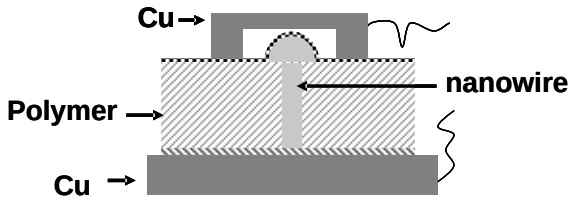

Figure 3. Schematic of experimental set up used for contacting electrically a single Au nanowire embedded in a polymer template.

The I-V characteristic measured at room temperature of a 145 nm diameter gold wire is displayed in Fig. 4 (a). The curve shows a linear symmetric form, which corresponds to an ohmic behavior. The resistance of the wire determined from the slope of the I-V curve amounts to 62 Ω. This metallic behavior was observed for all the wires investigated in this work. Recently, Lilley and Huang reported non-linear I-V curves for lithographically fabricated gold nanowires [18]. They attributed this observation to a surface contamination by oxygen and carbon. Thus, our results show a high quality of nanowires.

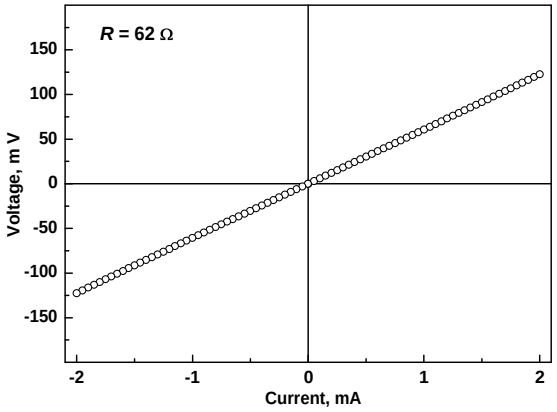

(a)

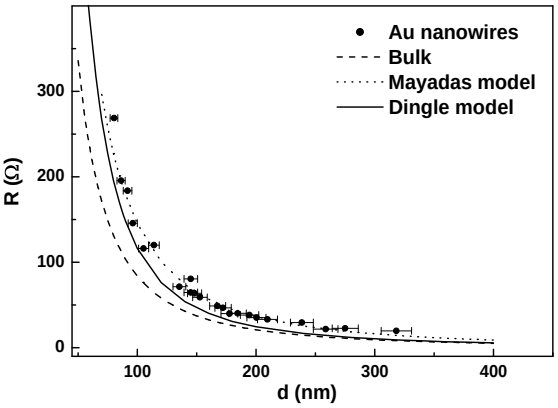

(b)

Figure 4 (a) A linear current-versus-voltage curve acquired at room temperature for a Au wire of diameter 145 nm. (b) The resistance of individual Au nanowires as a function of diameter. Dashed, dotted, and solid line represents the resistance calculated using the bulk resistivity of Au, Mayadas model, and Dingle model, respectively.

The values of the electrical resistance of individual gold nanowires measured at room temperature are displayed in Fig. 4(b) as a function of their diameter d. The uncertainties of the determination of the pore diameter constitute the

errors of d. This includes the errors of the template thickness, the specific electrical conductivity of the 1M KCl solution, and the measured current. The diameters were obtained by measuring the pore conductivity in a 1 M KCl solution at room temperature prior to wire deposition (experimental section). The dashed curve represents the resistance calculated using the specific electrical resistivity of bulk gold (ρ_{bulk} = 2.2 μΩ cm at 300 K [4, 19]). The resistance of the wires is higher than the classically determined value, and the deviation becomes more pronounced with diminishing diameter as reported in several previous studies for nanowires of different materials [3, 4, 12, 19]. The solid curve represents the resistance values calculated for 30 μm long cylindrical Au wires, taking into account completely inelastic scattering of the electrons at the wire surface according to the model of Dingle et al. [6]. In accordance with this model the electrical conductivity σ is given by following equations

k >> 1

$$\frac{\sigma}{\sigma_o} \approx 1-\frac{3}{4k}(1-p)+\frac{3}{8k^3}(1-p)^2\sum_1^\infty \frac{p^{\upsilon-1}}{v^2}$$

k << 1

$$\frac{\sigma}{\sigma_o} \approx \frac{1+p}{1-p}k-\frac{3k^2}{8}$$
$$\left[\frac{1+4p+p^2}{(1-p)^2}\left(\ln\frac{1}{k}+1.059\right)-(1-p)^2\sum_1^\infty v^3 p^{\upsilon-1}\ln v\right]-$$
$$\frac{2k^3}{15}\frac{\left(1+11p^2+p^3\right)}{(1-p)^3}$$

where σ_o is the bulk resistivity, and *k* is the ratio of the wire diameter d to the electronic mean free path l_e. The proportion of electrons that are not diffusively scattered from the wire surface is characterized by the so-called specularitiy parameter p. This is a phenomenological parameter that can take values between 0 and 1. If one assumes complete elastic scattering, the resulting, the R versus d curve corresponds thus to the resistance of the wires calculated with the bulk resistivity.

The resistivity attributed to electron scattering at the grain boundaries, as predicted by Mayadas and Shatzkes [8], is given by

$$\frac{\rho_o}{\rho} = 3\left[\frac{1}{3}-\frac{\alpha}{2}+\alpha^2+\alpha^3\ln\left(1+\frac{1}{\alpha}\right)\right]$$

with

$$\alpha = \frac{l_e}{D_g}\frac{R_g}{1-R_g}$$

Here D_g is the mean grain diameter and R_g denotes the reflection coefficient, representing the probability that an electron is reflected at a grain boundary. In accordance with this theory, three factors, namely, D_g, l_e and the reflectivity R_g determine the effect of grain boundary scattering on the resistivity. In our calculations we employed α as the fitting parameter. Inserting α = 0.5 provides the dotted curve in Fig. 4. The plots of the two models show that an enhanced resistivity due to scattering at grain boundaries is predicted, with contribution of scattering at the surface is almost negligible in the range of diameters reported here. The experimental values in Fig. 4 show resistances higher than predicted by the Dingle model even assuming total inelastic surface scattering. We attribute this to the relatively large size of wires with $d >> l_e$.

4. Conclusions

Single-pore membranes were prepared by irradiating polymer foils with exactly one swift heavy ion. By two-side etching, cylindrical pores of different diameters were created in these membranes which acted as templates for the growth of single Au nanowires. These wires were electrically contacted while embedded in the polymer matrix. The electrical measurements indicated that the wires have enhanced resistance as compared to the bulk metal that can be explained by the grain boundary scattering of conduction electrons. This method of contacting single nanowires offers the possibility of measuring transport properties of a wire without the use of lithographic processes or further manipulation while a wider range of growth conditions for the nanowires becomes accessible.

Acknowledgements

Support of the members of GSI materials research department during irradiation of samples at UNILAC is gratefully acknowledged.

References

[1] Y. Xia, P. Yang, Y. Sun, Y. Wu, B. Mayers, B. Gates, Y. Yin, F. Kim and H. Yan, Adv. Mater., **15** (2003) 353.

[2] C. R. Martin, Science, **266** (1993) 1961

[3] W. D. Williams and N. Giordano Phys. Rev. B, **33** (1986) 8146

[4] C. Durkan and M. E. Welland, Phys. Rev. B, **61** (2000) 14215.

[5] S. Datta (1995) Electronic Transport in Mesoscopic Systems, Cambridge University Press, Cambridge.

[6] R. B. Dingle, Proc. R. Soc., A **201** (1950) 545.

[7] K. Fuchs, Proc. Cambridge Philos. Soc., **34** (1938) 100.

[8] A. F. Mayadas and M. Shatzkes, Phys. Rev. **B1** (1970)1382.

[9] A. Bid, A. Bora and A. K. Raychaudhur, Phys. Rev. **B74** (2006) 35426.

[10] A. Satti, D. Aherne and D. Fitzmaurice, Chem. Mater., **19** (2007)1543.

[11] S. Valizadeh, M. Abid, F. Hernández-Ramírez, A. Romano Rodríguez, K. Hjort and J. Å. Schweitz, Nanotechnology, **17** (2006) 1134.

[12] T. W. Cornelius, M. E. Toimil-Molares, S. Karim and R. Neumann, J. Appl. Phys. **100** (2006)114307.

[13] M. E. Toimil-Molares, N. Chatanko, T. W. Cornelius, D. Dobrev, I. Enculescu, R. H. Blick and R. Neumann, Nanotechnology, **15** (2004) s201.

[14] P. Y. Apel, Y. E. Korchev, Z.Siwy, R. Spohr and M. Yoshida, Nucl. Instr. and Meth. In Phys. Res. B, **184** (2001) 337.

[15] S. Karim, M.E. Toimil-Molares, F. Maurer, G. Miehe, W. Ensinger, J. Liu, T. W. Cornelius and R. Neumann, Appl. Phys. A, **84** (2006) 403.

[16] J. Liu, J.L. Duan, M. E. Toimil-Molares, S. Karim, T. W. Cornelius, D. Dobrev, H. J. Yao, Y.M. Sun, M. D. Hou, D. Mo, Z. G. Wang, and R. Neumann, Nanotechnology **17** (2006) 1922.

[17] N. Chtanko, M. E. Toimil Molares, T. W. Cornelius, D. Dobrev and R. Neumann, J. Phys. Chem. B, **108** (2004) 9950.

[18] C. M. Lilley and Q. Huang, Appl. Phys. Lett., **89** (2006) 203114.

[19] E. J. Menke, M. A. Thompson, C. Xiang, L.C. Yang and R. M. Penner, Nat. Mater,. **5** (2006) 914.

This document was created with Win2PDF available at http://www.win2pdf.com.
The unregistered version of Win2PDF is for evaluation or non-commercial use only.
This page will not be added after purchasing Win2PDF.